Finding cycles in nonlinear autonomous discrete dynamical systems

D.Dmitrishin, A.Khamitova, A.Stokolos and M.Tohaneanu

Dedicated to Alexey Solyanik on his 55th birthday

Abstract The goal of this paper is to provide an exposition of recent results of the authors concerning cycle localization and stabilization in nonlinear dynamical systems. Both the general theory and numerical applications to well-known dynamical systems are presented. This paper is a continuation of [16].

1 Introduction

The problem of cycle detection is fundamental in mathematics. In this paper we will be mainly concerned with the problem of detecting cycles of large length in an autonomous discrete system $x_{n+1} = f(x_n)$. The standard approach is to consider the composition map $f_T(x) := f(...f(x)...)$ and then solve the equation $f_T(x) = x$. However, this approach does not work well even in some basic cases. For example, in the model case of the logistic map $f(x) = 4x(1-x)$ it leads to a polynomial equation of degree 2^T, and thus a relatively small cycle length T can give rise to very serious computational difficulties.

Dmitriy Dmitrishin
Odessa National Polytechnic University, 1 Shevchenko Ave., Odessa 65044, Ukraine e-mail: dmitrishin@opu.ua

Anna Khamitova and Alex Stokolos
Georgia Southern University, Statesboro, GA 30458, USA
e-mail: anna_khamitova@georgiasouthern.edu, astokolos@georgiasouthern.edu

MihaiTohaneanu
University of Kentucky,Lexington KY, 40506, USA e-mail: mihai.tohaneanu@uky.edu

The goal of this article is to suggest an alternative approach to the problem of cycle localization. In full generality the problem is very difficult and it is hard to believe that a universal technique could be developed. We thus start with a model case of non-linear autonomous discrete dynamical systems. The simplicity of the setting allows us to make some progress and to develop a feasible plan for further developments of the method. Since one fundamental tool of dynamics, often used for analyzing continuous time systems, is the reduction of continuous time flow to its Poincaré section, which is a discrete system, understanding the case of discrete systems is of great help in studying continuous systems also.

The core of the suggested method is the stabilization of the solutions by delayed feedback control (DFC) of a special type. We will briefly discuss a way to linearly stabilize the system in Section 4; however, it turns out that the linear DFC method has some obvious limitations regardless of the number of prehistory terms involved. In contrast, in the subsequent sections we will show that a certain nonlinear DFC schedule allows one to robustly stabilize chaotic solutions for any admissible range of parameters.

The methods we developed can be considered as chaos stabilization, and we believe they are of interest in other disciplines. Chaos theory is a part of modern Physics and the majority of the publications on chaos are in Physics literature; for instance, problems of stability have been discussed in [1-5], [8-12], [13, 24, 25, 27, 28, 32, 34, 36]. There are many specialists in chaos theory who are physicists, among whom we mention E. Ott, C. Grebogi, J.A. Yorke, K. Pyragas, P. Cvetanović etc. On the other hand, many biological systems exhibit chaotic behavior as well. A fundamental monograph of I.D. Murray [22] contains deep and advanced discussions and applications of the non-linear dynamical systems to models of population growth.

2 Settings

Consider the discrete dynamical system

$$x_{n+1} = f(x_n), \qquad f : A \to A,\ A \subset \mathbb{R}^m. \tag{1}$$

where A is a convex set that is invariant under f. Let us assume that the system has an unstable T-cycle $(x_1^*, ..., x_T^*)$. We define the cycle multipliers $\mu_1, ..., \mu_m$ as the zeros of the characteristic polynomial

$$\det\left(\mu I - \prod_{j=1}^{T} Df(x_j^*)\right) = 0. \tag{2}$$

We will assume that the multipliers are located in a region $M \subset \mathbb{C}$.

3 Stability analysis

A standard approach (c.f. [21]) to investigate stability with no delays is to construct a new map that has points of the cycle as equilibriums and then linearize about the equilibriums. Let us consider a system with time delay in a general form

$$x_{n+1} = F(x_n, x_{n-1}, ..., x_{n-\tau}), \qquad F : \mathbb{R}^m \to \mathbb{R}^m,\ \tau \in \mathbb{Z}_+. \tag{3}$$

We will study the local stability of a cycle $\{\eta_1, ..., \eta_T\}$ where $\eta_j \in \mathbb{R}^m$. In other words for all $n \geq \tau + 1$ the following equations are valid

$$\eta_{(n+1) \mod T} = F(\eta_{n \mod T}, \eta_{(n-1) \mod T}, ..., \eta_{(n-\tau) \mod T}).$$

where, slightly abusing notation, we assume that $T \mod T = T$.

We can now consider an auxiliary system with respect to the vector

$$z_n = \begin{pmatrix} z_n^{(1)} \\ z_n^{(2)} \\ \vdots \\ z_n^{(\tau+1)} \end{pmatrix} = \begin{pmatrix} x_{n-\tau} \\ x_{n-\tau+1} \\ \vdots \\ x_n \end{pmatrix}.$$

of size $m(\tau + 1)$:

$$z_{n+1} = \begin{pmatrix} z_{n+1}^{(1)} \\ z_{n+1}^{(2)} \\ \vdots \\ z_{n+1}^{(\tau+1)} \end{pmatrix} = \begin{pmatrix} z_n^{(2)} \\ z_n^{(3)} \\ \vdots \\ f(z_n^{(\tau+1)}, z_n^{(\tau)}, ..., z_n^{(1)}) \end{pmatrix}.$$

We can now rewrite (3) in the form

$$z_{n+1} = \mathcal{F}(z_n)$$

with $\mathcal{F} : \mathbb{R}^{m(\tau+1)} \to \mathbb{R}^{m(\tau+1)}$.

Let $\Psi(z) := \mathcal{F}(...\mathcal{F}(z)...)$ be $\mathcal{F}$ composed with itself T-times. We can now analyze the system

$$y_{n+1} = \Psi(y_n). \tag{4}$$

Let us periodically repeat the elements of the cycle:

$\{\eta_1, \eta_2, ..., \eta_T, \eta_1, \eta_2, ..., \eta_T, ...\}$. The first $\tau + 1$ elements of this sequence form a vector

$$y_1^* = \begin{pmatrix} \eta_1 \\ \eta_2 \\ \vdots \end{pmatrix}.$$

In the same way we define the vectors

$$y_2^* = \begin{pmatrix} \eta_2 \\ \eta_3 \\ \vdots \end{pmatrix}, \ \dots, \ y_T^* = \begin{pmatrix} \eta_T \\ \eta_1 \\ \vdots \end{pmatrix}.$$

It is clear that the vectors $y_1^*, ..., y_T^*$ are equilibria of the system (4).

The cycle $\{\eta_1, ..., \eta_T\}$ of the system (3) is asymptotically locally stable if and only if all equilibriums $y_1^*, ..., y_T^*$ of the system (4) are asymptotically locally stable.

For the equilibrium point y_1^* of the system (4) the Jacobi matrix is defined by the formula

$$D\Psi(y_1^*) = \prod_{j=1}^{T} D\mathcal{F}(y_j^*) \tag{5}$$

where the matrix $D\mathcal{F}(y_j^*)$ has size $m(\tau+1) \times m(\tau+1)$ and equals

$$D\mathcal{F}(y_j^*) = \begin{pmatrix} O & I & O & ... & O \\ O & O & I & ... & O \\ .... & & & & \\ O & O & O & ... & I \\ Q_1^{(j)} & Q_2^{(j)} & Q_3^{(j)} & ... & Q_{\tau+1}^{(j)} \end{pmatrix}. \tag{6}$$

Here the matrices O and I are the $m \times m$ zero and identity matrices. Further,

$$Q_r^{(j)} = \left. \frac{\partial f}{\partial z^{(r)}} \right|_{y_j^*}, \quad r = 1, ..., \tau+1; \ j = 1, ..., T,$$

i.e. the value of the derivative evaluated at the point y_j^*.

For all other equilibria y_j^* the Jacobi matrices $D\mathcal{F}(y_j^*)$ can be computed in the same manner, and

$$D\Psi(y_j^*) = D\mathcal{F}(y^*_{(T+j) \mod T}) \cdots D\mathcal{F}(y_j^*),$$

which can be obtained from (5) by a cyclic permutation of the factors. The eigenvalues of $D\Psi(y_j^*)$ thus coincide for all $j = 1, ..., T$ (see for example [20] for more details.)

If all eigenvalues of the matrix $D\Psi(y_j^*)$, which are the roots of the polynomial

$$\det\left(\lambda I - D\Psi(y_j^*)\right)$$

are less than one in absolute values then the cycle of the system (3) is locally asymptotically stable.

Note that in the scalar case $m = 1$ the matrices $D\mathcal{F}(y_j)$ are in Frobenius form, and the matrix (6) is a generalized form of the companion matrix. If the system has the special form (10) below, then the characteristic equation can be found explicitly by means of induction, see [14].

4 Linear Control

There is a common belief that a generalized linear control

$$u = -\sum_{j=1}^{N-1} \varepsilon_j \left(x_{n-j} - x_{n-j+1}\right) \tag{7}$$

can stabilize the equilibrium for the whole range of the admissible multipliers of the system (1). In this case $F(x_n, x_{n-1}, ..., x_{n-(N-1)T}) = f(x_n) + u$ and the characteristic equation for the system closed by the control (7) is $\chi_\mu(\lambda) = \prod_{j=1}^{m} \chi_{\mu_j}(\lambda)$, where $\chi_\mu(\lambda) := \lambda^N - \mu\lambda^{N-1} + p(\lambda)$ and

$$p(\lambda) = a_1\lambda^{N-1} + a_2\lambda^{N-2} + \cdots + a_N. \tag{8}$$

Here μ_j are cycle multipliers, i.e. the roots of the characteristic equation (2) of the open loop system, while the coefficients a_i and the gain ε_j are related by the bijection

$$\varepsilon_j = \sum_{k=j+1}^{N} a_k,\ j = 1, ..., N-1. \tag{9}$$

The proof can be done by the methods considered in the section 3 above. It is not trivial but similar to a non-linear scalar case [14].

In the case of real multipliers μ a careful application of Vieta's theorem implies that a necessary condition for the polynomials $\chi_\mu(\lambda)$ to be Schur stable is $1 - 2^N < \mu < 1$. It turns out [36] that for any fixed μ in this range there are coefficients that guarantee the stability of the polynomial $\chi_\mu(\lambda)$ for this given μ.

At this point, a natural question to ask is how robust the selected control can be, i.e. assuming that we are given the Schur-stable polynomials $\chi_\mu(\lambda)$, how much can we perturb the multipliers μ so that $\chi_\mu(\lambda)$ remain Schur-stable? More rigorously, the inquiry is the following:

What is the maximum length of a connected component of M?

In [18] we discovered a remarkable fact - the answer to the above question is 4 regardless of how large N is. Below is an idea of the proof.

4.1 Solyanik visualisation

The polynomial $\chi_m(\lambda)$ is quite complicated and difficult to study directly. Alexey Solyanik [29] suggested a remarkable way to visualize the situation. Namely, $\chi_\mu(\lambda)$ is a stable polynomial if and only if $\chi_\mu(\lambda) = \lambda^N - \mu\lambda^{N-1} + p(\lambda) \neq 0$ for $|\lambda| \geq 1$ or

$$\frac{1}{\mu} \neq \frac{\frac{1}{\lambda}}{1 + \frac{p(\lambda)}{\lambda^N}} \Rightarrow \frac{1}{\mu} \neq \frac{z}{1 + q(z)} =: \Phi(z),\ |z| \leq 1.$$

where $z = \frac{1}{\lambda}$ and $q(z) = \frac{p(\lambda)}{\lambda^N}$. Therefore χ_μ is Schur stable if and only if $1/\mu \notin \Phi(\bar{\mathbb{D}})$, where $\mathbb{D} = \{z : |z| < 1\}$. This can be rewritten as $\mu \in (\bar{\mathbb{C}} \backslash \Phi(\bar{\mathbb{D}}))^*$, where $z^* := 1/\bar{z}$ is an inversion. The above formula reduces the problem of stability to the problem of verifying whether μ is in the above set, which is still difficult, but more manageable.

4.2 Köbe Quarter Theorem application.

Now, let expand $\Phi(z)$ in a power series $\Phi(z) = z + a_2 z^2 + a_3 z^3 + ...$ in $\mathbb{D}$. If Φ is univalent, then by the Köbe Quarter Theorem $\frac{1}{4}\mathbb{D} \subset \Phi(\mathbb{D})$ and therefore

$$\left|\frac{1}{\mu}\right| > \frac{1}{4} \Rightarrow |\mu| < 4.$$

We were able to get in [18] a generalization of the Köbe Quarter Theorem which allowed us to obtain the result mentioned above. We also remark that the inequality above explains the value 4 mentioned in the previous section.

Finally, it was proved in [18] that *if the diameter of the set of multipliers is larger than 16, or the diameter of any of its connected component is larger than 4, then for any N there is no control* (7) *that stabilizes equilibria of the system* (1) *for all admissible parameters of the system.*

The other obvious problem with the linear control is that the close-loop system can have solutions that are outside the domain of the map, i.e. the convex invariant set for the open-loop system is not necessarily an invariant set for the closed-loop system. In Fig.1 below the solution to the logistic system closed by the control $u = -0.01(x_n - x_{n+1})$ with $x_0 = 0.7501$ is displayed. Note that $x_0 = 0.75$ is an equilibrium for a logistic map while a little perturbation produces a solution that blows up after 30 iterations.

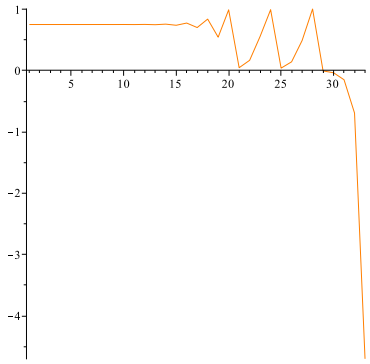

Fig. 1: Logistic close-loop system.

These two basic obstacles - the range for of the close-loop system and the limited rage for the connected component for the multiplier - justify the introduction of the non-linear controls.

5 Average non-linear control

Typically, an arbitrarily chosen initial value x_0 produces a chaotic solution, i.e. we observe strong oscillations. An efficient way to kill oscillations is averaging, as can be readily seen in the summability of many trigonometric series. So, we decided to consider a new system

$$x_{n+1} = \sum_{k=1}^{N} a_k f(x_{n-kT+T}), \qquad \sum_{k=1}^{N} a_k = 1. \tag{10}$$

It is useful to rewrite the system as $x_{n+1} = f(x_n) + u_n$, where

$$u_n = -\sum_{j=1}^{N-1} \varepsilon_j \left(f\left(x_{n-jT+T}\right) - f\left(x_{n-jT}\right)\right), \tag{11}$$

where a_k and ε_k are in one-to-one correspondence as in (9).

We can now see that (10) in fact is the system (1) closed by the control (11). In this case the convex invariant set for the open-loop system is also invariant for the closed-loop system. We also remark that $u_n = 0$ for cycle points of period T, which implies that the closed-loop system $x_{n+1} = f(x_n) + u_n$ preserves the T-cycles of the initial one, which is very important for us.

5.1 Stability analysis

The characteristic equation for the system (10) can be written in a remarkably useful form

$$\prod_{j=1}^{m}\left[\lambda^{T(N-1)+1} - \mu_j\left(\sum_{k=1}^{N} a_k\lambda^{N-k}\right)^T\right] = 0, \quad \mu_j \in M,\ j = 1, ..., m.$$

Here μ_j are the multipliers of the open loop system (1). The proof for the scalar case $m = 1$ can be found in [14], and the vector case can be done in a similar way. Denote

$$\phi(\lambda) := \lambda^{T(N-1)+1} - \mu\left(\sum_{k=1}^{N} a_k\lambda^{N-k}\right)^T,$$

$$q(z) = \sum_{j=1}^{N} a_j z^{j-1} \quad \text{and} \quad z = \frac{1}{\lambda}.$$

Then $\phi(\lambda) = 0$ is equivalent to $\mu^{-1} = z\,(q(z))^T$. So, if

$$F_T(z) := z\,(q(z))^T \tag{12}$$

then the inclusion

$$M \subset (\bar{\mathbb{C}}\backslash F_T(\bar{\mathbb{D}})^* \tag{13}$$

guarantees the local asymptotic stability of the cycle with multipliers in the set M. The inclusion (13) is the Solyanik visualization in this setting.

We are thus left with the following problem in geometric complex function theory: *given a set M containing all the multipliers, find a properly normalized polynomial map $z \to F_T(z)$ such that $M \subset \left(\bar{\mathbb{C}}\backslash F_T(\bar{\mathbb{D}})\right)^*$.*

Since in the simplest case $x_{n+1} = \mu x_n$ the solution $x_n = C\mu^n$ is exponentially blowing up for $\mu > 1$ there is no way to stabilize the case when one of the multipliers satisfies $\mu > 1$ by only using the small gain (11). Therefore we will consider only negative real multipliers, and in the complex case we will assume that M is disjoint from $[1, \infty)$. We also remark that the cycle is already stable if the multipliers are in $(-1, 1)$ or more generally in the unit disc $\mathbb{D}$ of the complex plane $\mathbb{C}$.

It is natural to expect that the stability will be getting worse if the set M is close to the half axis $[1, \infty)$. Below we will see several examples supporting this thesis.

Since $((0, \infty)\backslash(0, 1])^* = (0, 1)$, and (0,1) is the largest admissible range for real positive multipliers, the best case scenario for us is a polynomial whose image of the unit disc looks like a narrow neighborhood of $(0, 1]$. Solyanik [29] suggested as an example of such an object a famous Alexander polynomial - the polynomial with the coefficients $a_k = 1/k$, properly normalized [1]. The corresponding set $(\bar{\mathbb{C}}\backslash F_T(\bar{\mathbb{D}})^*$ has a cardioid type shape and for a large N can cover any given point except for the real numbers $z \geq 1$. We refer the reader to Fig.2, where the image of the unit disc under the Alexander polynomial map is the interior of the inner (orange) curve, and the set $(\bar{\mathbb{C}}\backslash F_T(\bar{\mathbb{D}})^*$ is the interior of the outer (green) curve.

We thus know that theoretically there is a way to stabilize equilibria with any multipliers outside $[1, \infty)$ by the control (11). However, the length of the prehistory is growing exponentially with the magnitude of the multiplier. In Fig.2 the largest multiplier which can be covered has a magnitude 15, while the length of the prehistory is 20,000. We are thus led to the problem of finding the optimal coefficients a_j so that for a given set of multipliers M the prehistory N is as small as possible.

It turns out that in the case of multipliers with negative real part the number N can be shown to be much smaller, of only polynomial growth with respect to the size of the multipliers, which is of practical use. This will be explored in the subsequent sections.

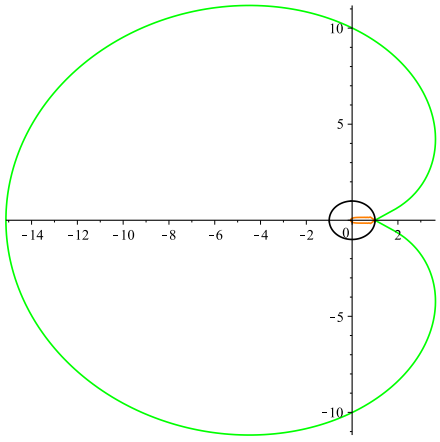

Fig. 2: Image of $F(\mathbb{D})$ with the Alexander polynomial $F(z)$, $N = 20000$.

6 Optimization problem

Let us look first at the case when the multipliers lie on the half-axis $(-\infty, 1)$. In this case the problem of stabilization can be reduced to the following optimization problem: find

$$I_N^{(T)} = \sup_{\sum_{j=1}^N a_j = 1} \min_{t\in[0,\pi]} \left\{ \Re\left(F_T(e^{it})\right) : \Im\left(F_T(e^{it})\right) = 0 \right\}.$$

Technically speaking, this leads to a disconnected set of multipliers, as the boundary of $(\bar{\mathbb{C}}\backslash F_T(\bar{\mathbb{D}})^*$ will be tangent to the real axis (see, for example, Fig. 4 below). However, there is an easy trick to get rid of the tangent points: given $\epsilon > 0$ the polynomial $F_T^\epsilon(z) = (1+\epsilon)^{-1}(F_T(z) + \epsilon z)$ satisfies

$$\min_{t\in[0,\pi]} \left\{ \Re\left(F_T^\epsilon(e^{it})\right) : \Im\left(F_T^\epsilon(e^{it})\right) = 0 \right\} > I_N^{(T)} - \epsilon.$$

and does not intersect the real axis except for $t = 0$ and $t = \pi$. Since $\lim_{\epsilon\to 0} F_T^\epsilon(z) = F_T(z)$, one can use the coefficients of the polynomials $F_T(z)$ instead of $F_T^\epsilon(z)$ in computer simulations. In particular, it is done below.

It can be shown that for the closed-loop system a robust stabilization (i.e. by the same control for all $\mu \in (-\mu^*, 1)$) of any T-cycle is possible if

$$(\mu^*) \cdot |I_N^{(T)}| \le 1. \tag{14}$$

By duality, for any $\mu^* \ge 1$ a robust stabilization of T-cycle in the closed-loop system is possible if $N \ge N^*$, where N^* is the minimal integer N such that (14) holds. Formula (14) provides a practical criterion for the choice of N given μ^* and T.

7 Real Multipliers, optimal polynomials for T=1

It was proved in [15] (see also [16]) that given N the largest μ such that

$$(-\mu, 1) \subset (\bar{\mathbb{C}}\backslash F_1(\bar{\mathbb{D}})^*$$

can be achieved if the coefficients of $q(z)$ in (12) are the coefficients of a polynomial related to the well-known Fejér polynomial, namely

$$a_j = 2\tan\frac{\pi}{2(N+1)}\left(1 - \frac{j}{N+1}\right)\sin\frac{\pi j}{N+1}, \quad j = 1, ..., N. \tag{15}$$

Moreover, any N such that

$$\mu \cdot \tan^2 \frac{\pi}{2(N+1)} \leq 1$$

allows stabilization and *this inequality is sharp*.

For the choice $N = 12$ we display the image $F_1(\mathbb{D})$ and the maximal multiplier set M that allows for stability in Fig.3 and Fig. 4.

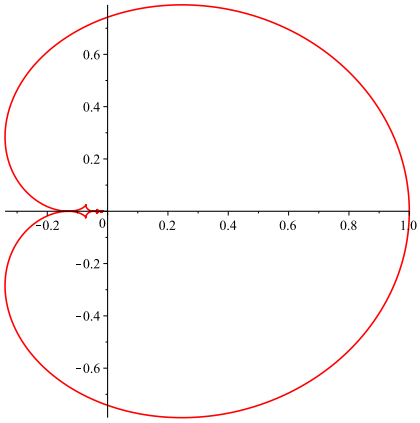

Fig. 3: $F_1(\mathbb{D})$, N=12.

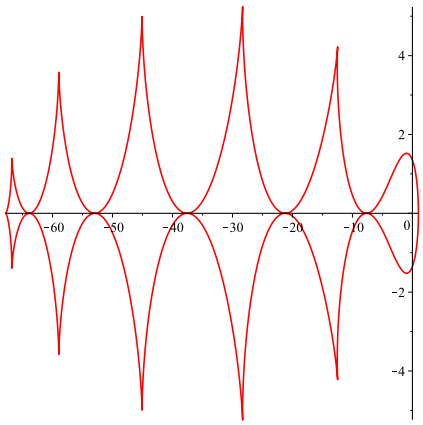

Fig. 4: $M = (\bar{\mathbb{C}} \backslash F_1(\bar{\mathbb{D}})^*$.

Note that for $N = 12$ the boundary for the multiplier is

$$\mu \cdot \tan^2 (\pi/26) \leq 1.$$

That implies that $\mu \leq 68$ which is easy to see in Fig. 4.

8 Real Multipliers, optimal polynomials for T=2

It was proved in [17] (see also [16]) that given N the largest μ such that

$$(-\mu, 1) \subset (\bar{\mathbb{C}} \backslash F_2(\bar{\mathbb{D}})^*$$

can be achieved if the coefficients of $q(z)$ in (12) are coefficients related to the Fejér kernel of order $2N$

$$a_j = \frac{2}{N}\left(1 - \frac{2j-1}{2N}\right), \qquad j = 1, ..., N. \tag{16}$$

Moreover, any N such that

$$\mu \cdot \frac{1}{N^2} \leq 1$$

allows stabilization of a 2-cycle and *this inequality is sharp*.

For the choice $N = 12$ we display the image $F_1(\mathbb{D})$ and the maximal multiplier set M that allows for stability in Fig.5 and Fig. 6.

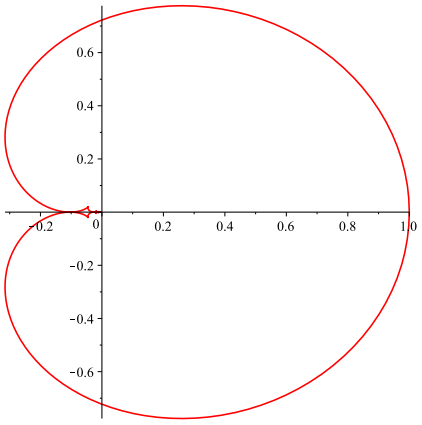

Fig. 5: $F_2(\mathbb{D})$, N=12

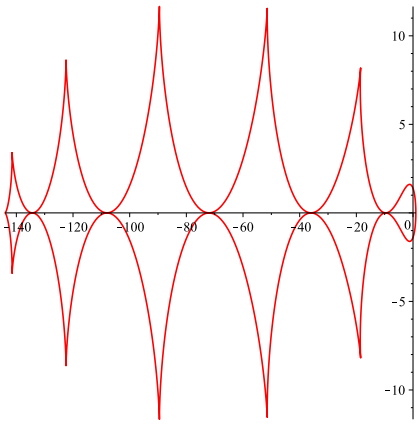

Fig. 6: $M = (\bar{\mathbb{C}} \backslash F_2(\bar{\mathbb{D}})^*$

Note that for $N = 12$ the boundary for the multiplier is $\mu \cdot \frac{1}{12^2} \leq 1$. That implies that $\mu \leq 144$ which is easy to see in Fig.6.

9 Real multipliers, quasi-optimal polynomials, $T \geq 3$

The case $T \geq 3$ is much more difficult compare to the cases $T = 1, 2$. We were unable to employ harmonic analysis technique and had to use complex analysis methods. Remarkably enough, we were able to construct a family of polynomials that are optimal for $T = 1, 2$ and that produce the expected estimate for the multiplier range if $T \geq 3$.

Define the set of points

$$t_j = \frac{\pi(\sigma + T(2j-1))}{\tau + (N-1)T}, \quad j = 1, .., \frac{N}{2} \text{ (N-even)}, \left(\frac{N-1}{2} \text{ (N-odd)} \right)$$

and the generating polynomials

$$\eta_N(z) = z(z+1) \prod_{j=1}^{\frac{N-2}{2}} (z - e^{it_j})(z - e^{-it_j}), \quad \text{N-even;}$$

$$\eta_N(z) = z \prod_{j=1}^{\frac{N-1}{2}} (z - e^{it_j})(z - e^{-it_j}), \quad \text{N-odd.}$$

Writing $\eta_N(z)$ in a standard form

$$\eta_N(z) = z\sum_{j=1}^{N} c_j z^{j-1}$$

we can define the following three-parameter family of polynomials

$$q(z,T,\sigma,\tau) = K\sum_{j=1}^{N}\left(1-\frac{1+(j-1)T}{2+(N-1)T}\right)c_j z^{j-1}, \tag{17}$$

where K is a normalization factor that makes $q(1,T,\sigma,\tau)=1$. In the particular case $\sigma=\tau=2$ K is given by

$$\frac{1}{K} = 2^{\frac{N-2}{2}}\prod_{j=1}^{\frac{N-2}{2}}(1-\cos t_j), \quad N \text{ even},$$

and

$$\frac{1}{K} = 2^{\frac{N-3}{2}}\prod_{j=1}^{\frac{N-1}{2}}(1-\cos t_j), \quad N \text{ odd}.$$

The polynomials (17) are substitutes for $q(z)$ in (12) and play the same role in the $T\geq 3$ scenario as Fejér polynomials do in the cases $T=1,2$. Because of that we call them quasi-optimal.

For any T and N, by choosing $\sigma=\tau=2$ the relation (13) is valid for

$$\mu\left(\frac{T}{2+(N-1)T}\prod_{j=1}^{\frac{N-2}{2}}\cot^2\frac{t_j}{2}\right)^T < 1, \text{ N-even},$$

and

$$\mu\left(\prod_{j=1}^{\frac{N-1}{2}}\cot^2\frac{t_j}{2}\right)^T < 1, \text{ N-odd}.$$

Moreover, for large N the left hand side in the above inequalities is approximately

$$\frac{\mu}{N^2}\left(\pi^{\frac{2-T}{T}}\left(\Gamma\left(\frac{T+2}{2T}\right)\right)^2\right)^T \sim \pi^2\frac{\mu}{N^2}, \qquad T\to\infty.$$

The proof is work in preparation by the authors [19].

We conjecture that the coefficients we have found are actually optimal.

Conjecture A: *Assume that N and T are given. Then the largest μ such that*

$$(-\mu, 1) \subset (\bar{\mathbb{C}} \backslash F_T(\bar{\mathbb{D}})^*$$

has a magnitude proportional to N^2 and is achieved by picking $q(z)$ in (12) to be $q(z, T, 2, 2)$.

In favor of this conjecture are numeric simulations and the fact that for $T = 1, 2$ the new family coincides with the polynomials that are optimal. Moreover, Figures 7,9 and 8,10 are remarkably similar to Figures 3,5 and 4,6 which correspond to the cases $T = 1, 2$.

10 Examples

10.1 Example of a quasi-optimal polynomial for $T = 3, N = 5$

Let us consider a numeric example $T = 3, N = 5$. In this case $t_1 = 5\pi/14$ and $t_2 = 11\pi/14$. The generating polynomial is

$$\eta(z) = z + 2(\cos\frac{3\pi}{14} - \sin\frac{\pi}{7})z^2 + 2(1 - \cos\frac{\pi}{7} + \sin\frac{\pi}{14})z^3 + 2(\cos\frac{3\pi}{14} - \sin\frac{\pi}{7})z^4 + z^5.$$

The normalized factor is

$$K = \frac{1}{2}\left(1 - \cos\frac{5\pi}{14}\right)^{-1}\left(1 - \cos\frac{11\pi}{14}\right)^{-1} = 0.496...$$

To get the region for the locations of μ one needs first to build a covering polynomial

$$F_3(z) = z(q(z, 3, 2, 2))^3 = K^3 z\left(\frac{13}{14} + \frac{10}{7}(\cos\frac{3\pi}{14} - \sin\frac{\pi}{7})z + \right.$$

$$\left.(1 - \cos\frac{\pi}{7} + \sin\frac{\pi}{14})z^2 + \frac{4}{7}(\cos\frac{3\pi}{14} - \sin\frac{\pi}{7})z^3 + \frac{1}{14}z^4\right)^3.$$

See Fig.7. Then take the inverse and get the region displayed in Fig.8, where the range for the multiplier is $\mu \in (-33, 1)$. Using the above polynomials one can get the estimates $I_5^{(3)} \geq -0.03$. We conjecture that these values are optimal.

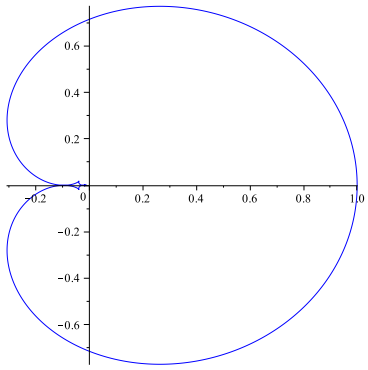

Fig. 7: $F_3(\mathbb{D})$, N=5.

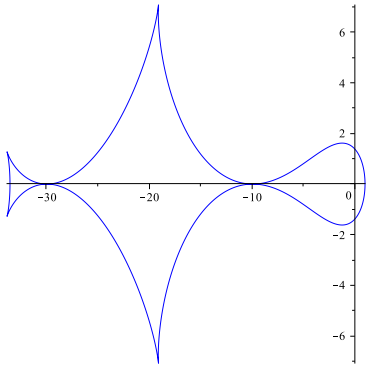

Fig. 8: $(\bar{\mathbb{C}}\backslash F_3(\bar{\mathbb{D}})^*$.

10.2 Example of 8-cycle in logistic equation

As an example of an application of the above method let us consider the logistic equation

$$x_{n+1} = 4x_n(1 - x_n). \tag{18}$$

It is well known that it has cycles of any length and that the cycles are unstable.

Consider the problem of *finding cycles of length 8*. Fig.9 displays the polynomial images of the unit disc $F_8(\mathbb{D})$ with the quasi-optimal polynomial of degree 12. Fig.10 displays the inverse image $(\bar{\mathbb{C}}\backslash F_8(\bar{\mathbb{D}})^*$.

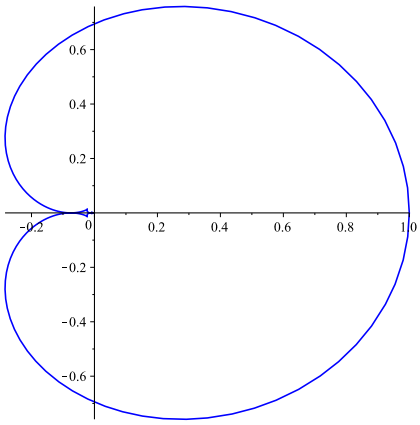

Fig. 9: $F_8(\mathbb{D})$, N=12

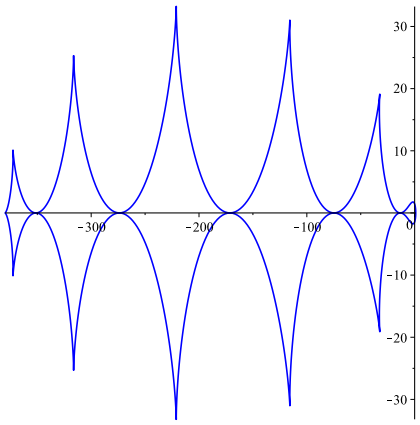

Fig. 10: $(\bar{\mathbb{C}}\backslash F_8(\bar{\mathbb{D}})^*$

To do that let us consider the system (18) and close it by the control

$$u_n = -\sum_{j=1}^{N-1} \varepsilon_j (f(x_{n-8j+8}) - f(x_{n-8j})).$$

We provide numeric simulation with the 8-cycle control above applied to the standard logistic equation. Fig.11 below reveals the existence of two 8-cycles. Moreover, the size of the control u_n goes to 0 as $n \to \infty$, so it provides an increasingly better approximation to the initial system. For $n \geq 9000$, for example, the control $|u_n| \leq 0.00002$, so we can obtain the value of the points of the two 8-cycles from Fig.11 up to the fifth decimal:

{0.2518;0.7535;0.7429;0.7640; 0.7213;0.8042;0.6299;0.9325}, and

{0.3408;0.8987;0.3642;0.9262;0.2733;0.7944;0.6533;0.9059}.

By increasing the number of iterations n one can get more digits in the cycle.

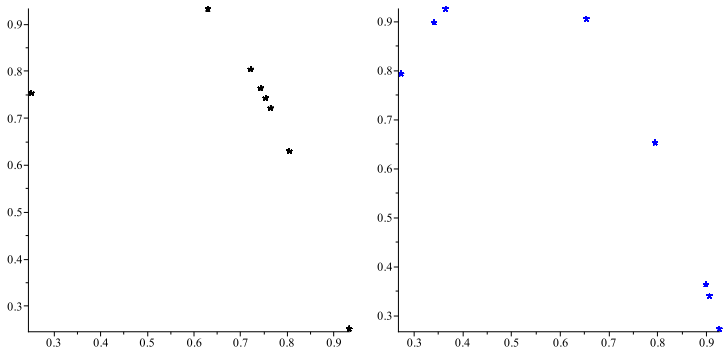

Fig. 11: Two 8-cycles in logistic equation on (x_{n-1}, x_n) plane

The subtlety of the situation is well illustrated by the fact that knowledge of a point on a cycle does not guarantee that the whole cycle can be found numerically by the iterative procedure (18) because of chaotic behavior of the solutions to (18). Fig.12 demonstrates what happens when we plug in $x_0 = 0.2518$ in (18). Since the system is chaotic, the numerical simulations do not reveal the existence of the 8-cycle. On the other hand, after adding an 8-cycle control the solutions exhibit 8-periodicity, see Fig.13.

Let us note that the standard approach would be to search for equilibria of the 8-folded composition of the logistic map. However this new map is a polynomial of degree 2^8 and therefore one should consider 512 roots on the interval [0,1]. Identifying those roots is a serious practical problem.

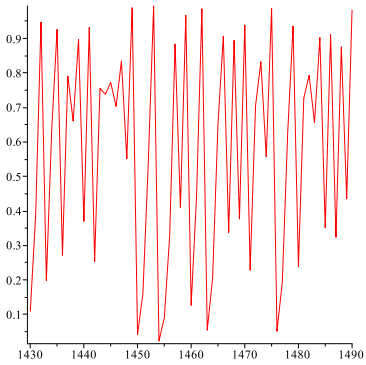

Fig 12: Dynamics of logistic equation with $x_0 = 0.2518$.

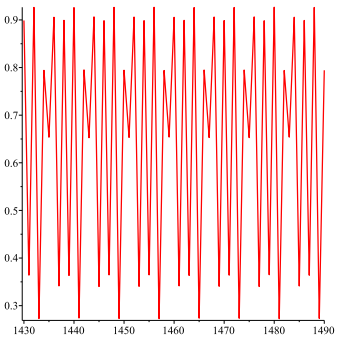

Fig 13: Dynamics of the solution in the closed-loop system with $x_0 = 0.2518$.

11 Complex Multipliers, $\Re(\mu) < 0$.

11.1 Complex Multipliers, case of equilibrium

Let us assume that $\mu \in \{\Re(z) < 0\} \cup \{|z| < 1\}$. Note the we consider the unit disk because if eigenvalues are in the unit disk, we have stability without any control added.

This domain may be considered as a union of the domains $M_R := \{|z + R| < R\} \cup \{|z| < 1\}$. If $R = N/2$ then choosing the polynomial map

$$F(z) = \frac{2}{N} \sum_{j=1}^{N} (1 - \frac{j}{N+1}) z^j$$

we can guarantee that the image of the unit disc will be to the right of the line $\Re(z) = -1/N$. Therefore, $M_{N/2}$ will be included in $\left(\bar{\mathbb{C}} \backslash F(\bar{\mathbb{D}})\right)^*$. We illustrate this in Fig. 14,15.

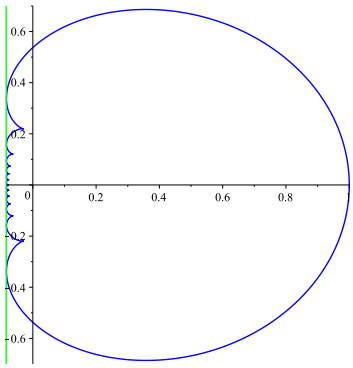

Fig: 14: $F(\mathbb{D})$, N=12

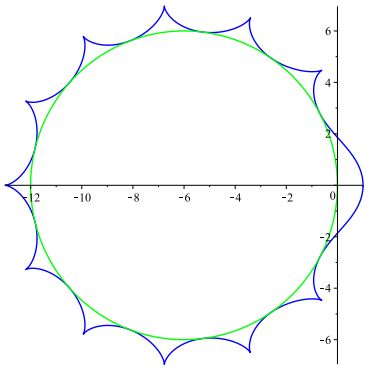

Fig. 15: $\left(\bar{\mathbb{C}}\backslash F(\bar{\mathbb{D}})\right)^*$.

11.2 Burgers map

As an example of an application let us consider the well-known Burgers map

$$\begin{cases} x_{n+1} = & 0.75x_n - y_n^2, \\ y_{n+1} = & 1.75y_n - x_n y_n. \end{cases}$$

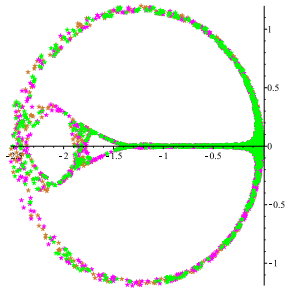

Fig. 16: Chaos

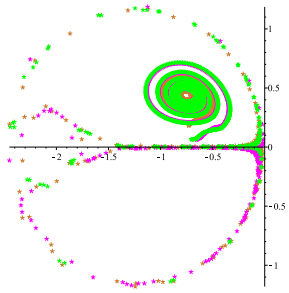

Fig. 17: Equilibrium, N=55

Here different colors correspond to different initial values. This plot as well as several plots below are in the (x_n, x_{n+1}) coordinate plane. We can see that after adding the nonlinear control an equilibrium point is clearly revealed in Fig. 17.

11.3 Arnold cat map

As another example, let us consider the famous Arnold cat map

$$\begin{cases} x_{n+1} = & (x_n + y_n) \mod 1, \\ y_{n+1} = & (x_n + 2y_n) \mod 1. \end{cases}$$

It is not globally smooth, so it is unlikely that our method will stabilize the equilibrium. However, it still has a regularizing effect on the dynamics, as can be seen in the pictures below. It would be interesting to understand why different orbits, corresponding to different colors, end up being separated by the nonlinear control, see Fig.20.

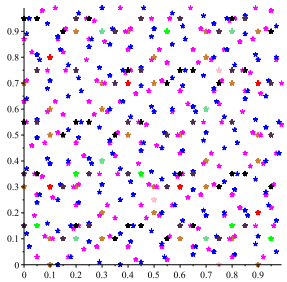

Fig. 18: Chaos

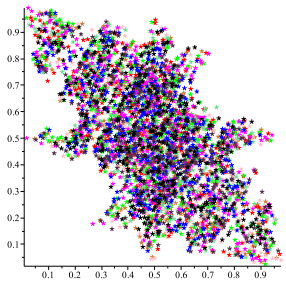

Fig. 19: T=1, N=3

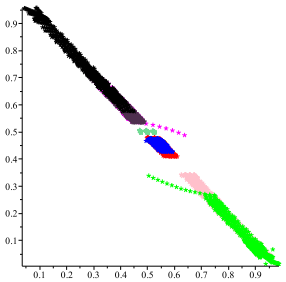

Fig. 20: T=1, N=50

11.4 Ikeda 3D map

Let us also look at the 3D Ikeda map

$$\begin{cases} x_{n+1} = & 1 + 0.9\left(x_n \cos\left(0.4 - \frac{6}{1+z_n^2}\right) - y_n \sin\left(0.4 - \frac{6}{1+z_n^2}\right)\right), \\ y_{n+1} = & 0.9\left(x_n \sin\left(0.4 - \frac{6}{1+z_n^2}\right) + y_n \cos\left(0.4 - \frac{6}{1+z_n^2}\right)\right), \\ z_{n+1} = & \sqrt{(x_n-1)^2 + y_n^2}. \end{cases}$$

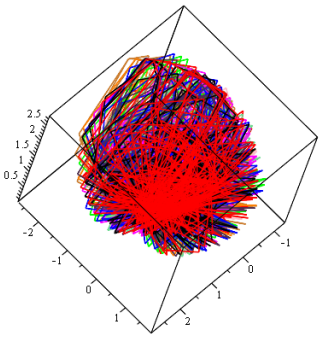

Fig. 22: Chaos

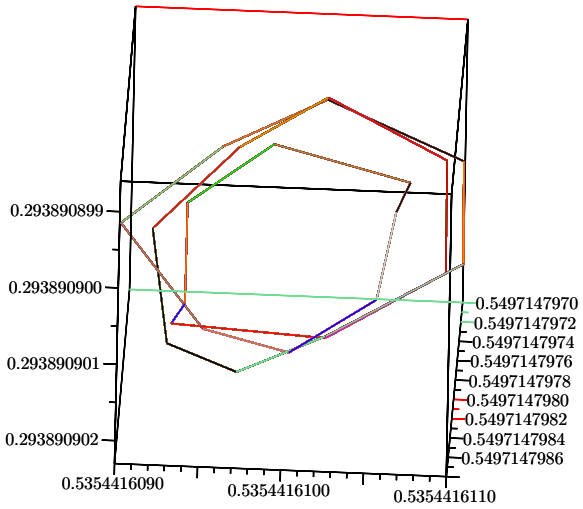

Fig. 23: Equilibrium, N=3.

One again notices an equilibrium, whose first few digits in the decimal expansion are $(0.5354416, 0.5497147, 0.2938909)$.

11.5 Complex Multipliers, $\Re(z) < 0$, $T \geq 2$

We illustrate the case of cycles of length 8, i.e. N=12, T=8., in Fig.23 and Fig.24. Here we use $F_T(z) = z\,(q(z,T,1,1))^T$.

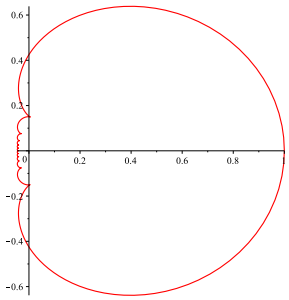

Fig. 23: $F_8(\mathbb{D})$, N=12

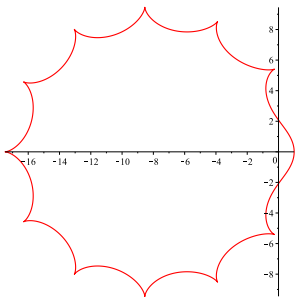

Fig. 24: $(\bar{\mathbb{C}}\backslash F_8(\bar{\mathbb{D}})^*$

In the following few subsections we illustrate how 4-cycles become visible after adding the nonlinear control.

11.6 Hennon map, T=4

Let us consider the Hennon map

$$\begin{cases} x_{n+1} = & 1 - 1.4x_n^2 + y_n, \\ y_{n+1} = & 0.3x_n. \end{cases}$$

Note the appearance of 4-cycles after adding a nonlinear control.

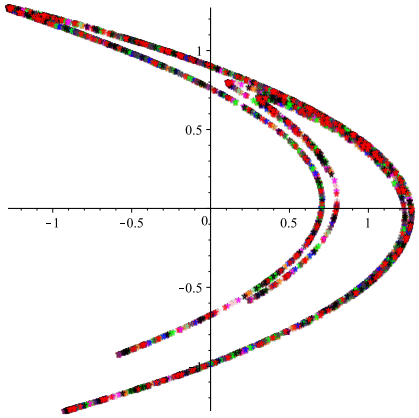

Fig. 25: Chaos

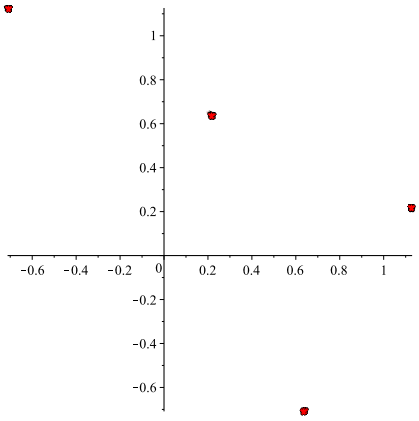

Fig. 26: 4-cycle, N=10.

11.7 Ikeda map, T=4

The 2D Ikeda map is given by

$$\begin{cases} x_{n+1} = & 1 + 0.9\left(x_n \cos\left(0.4 - \frac{6}{1+x_n^2+y_n^2}\right) - y_n \sin\left(0.4 - \frac{6}{1+x_n^2+y_n^2}\right)\right), \\ y_{n+1} = & 0.9\left(x_n \sin\left(0.4 - \frac{6}{1+x_n^2+y_n^2}\right) + y_n \cos\left(0.4 - \frac{6}{1+x_n^2+y_n^2}\right)\right), \end{cases}$$

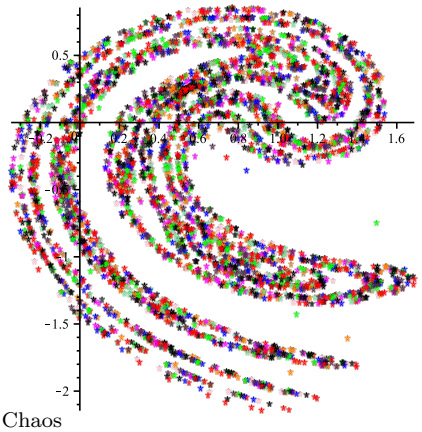

Fig. 27: Chaos

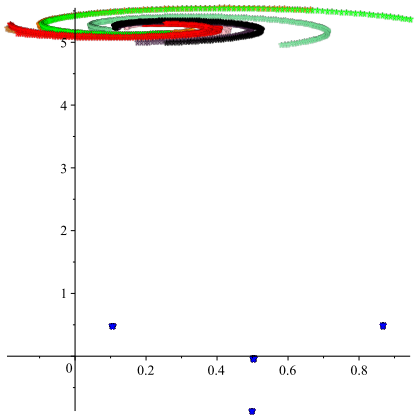

Fig. 28: 4-cycle, N=6.

11.8 Lozi map, T=4

The Lozi map is defined by the system

$$\begin{cases} x_{n+1} = 1 - 1.7|x| + 0.5y, \\ y_{n+1} = x_n. \end{cases}$$

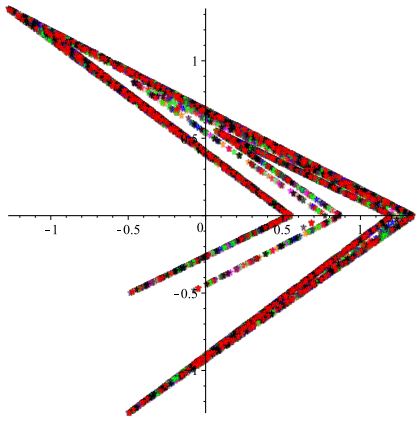

Fig. 29: Chaos

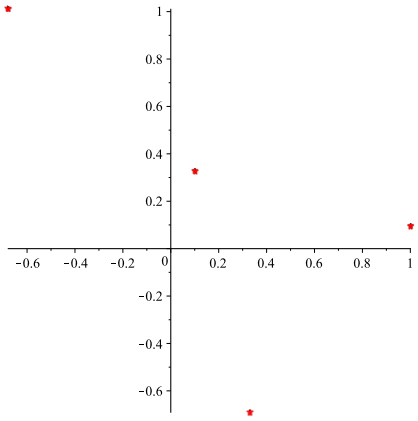

Fig. 30: 4-cycle, N=40

11.9 Holmes cubic map, T=4

The Holmes cubic map is defined by the system

$$\begin{cases} x_{n+1} = y_n \\ y_{n+1} = -0.2x + 2.77y - y^3. \end{cases}$$

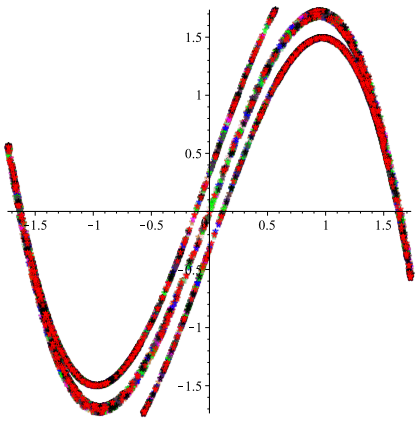

Fig. 31: Chaos

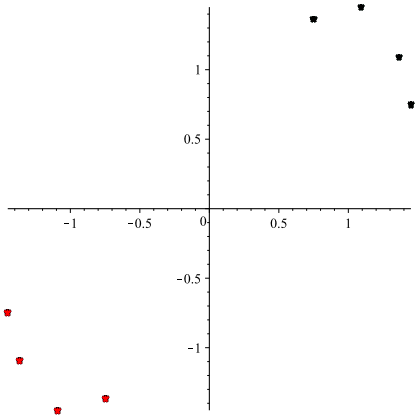

Fig. 32: Two 4-cycles, N=18.

11.10 Baker's map, T=2

Baker's map is defined by the system

$$\begin{cases} x_{n+1} = 2x_n - \lfloor 2x_n \rfloor, \\ y_{n+1} = \frac{1}{2}(y + \lfloor 2x_n \rfloor). \end{cases}$$

It is yet another example of globally non-smooth map in addition to Arnold cat considered above. It is remarkable that in both case one can observe separation of initial values, thus a regularization of chaotic behavior.

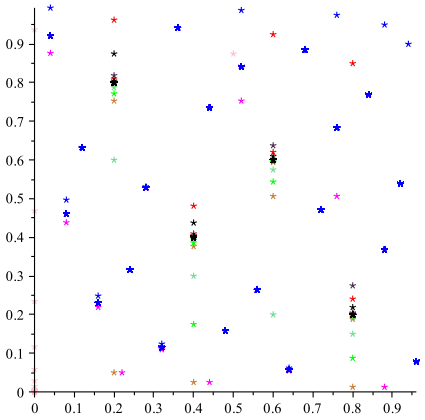

Fig. 33: Chaos.

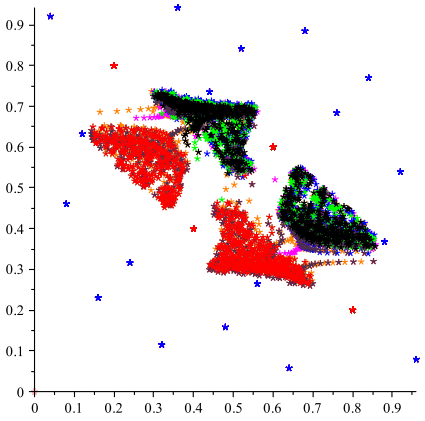

Fig. 34: T=2, N=20.

12 Complex multipliers, $\Re(\mu) > 0$

In this case the worst possible scenario consists of having real multipliers. Recall that even in the simplest system $x_{n+1} = \mu x_n$ the solution $x_n = C\mu^n$ blows up exponentially and our control cannot stabilize it, since there are no oscillations present. Therefore, it is natural to expect that the required N will grow very fast as the set of multipliers M gets close to the real line. The Alexander polynomials illustrate this hypothesis very well.

One piece of good news is that now we can use $q(z, T, \sigma, \tau)$ instead of Alexander polynomials. There is a choice of the parameters that allows the set (13) to cover any part of the region $\mathbb{C}\backslash[1, \infty)$ right to the imaginary axis as $N \to \infty$. The sets look like the angel wings in Fig.36 below, or like the dragonfly wings in Fig.38. The value of $N = 503$ is, of course, huge, but it is much better compare to $N = 20,000$ for Alexander polynomials. The values for N are selected to highlight the difference between the case of negative real part multipliers, where $N = 12$ suffices for very negative values of the real part, and the positive real part multipliers, where even for a relatively small multipliers a very large value of N is required.

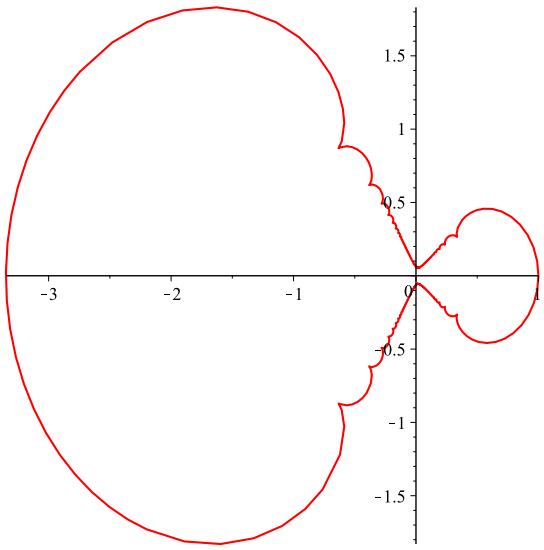

Fig. 35: $F_1(\bar{\mathbb{D}})$, $\sigma = 1.2$, $\tau = 0.5$, N=503.

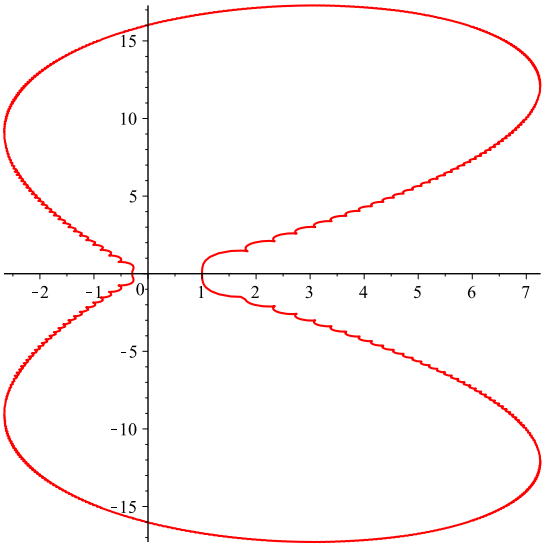

Fig. 36: $(\bar{\mathbb{C}}\setminus F_1(\bar{\mathbb{D}})^*$

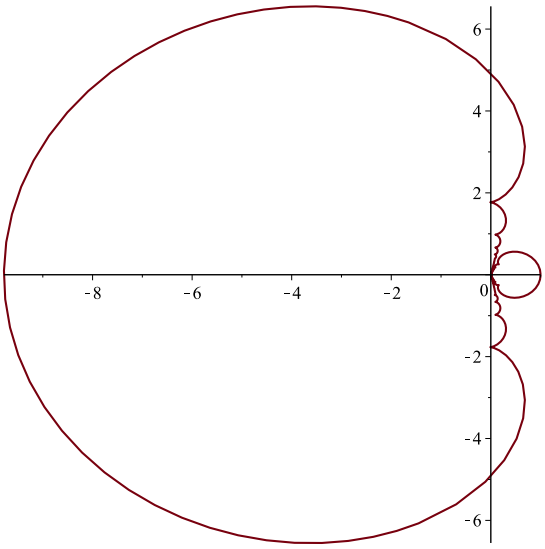

Fig. 37: $F_1(\bar{\mathbb{D}})$, $\sigma = 1.9$, $\tau = 0.75$, N=503.

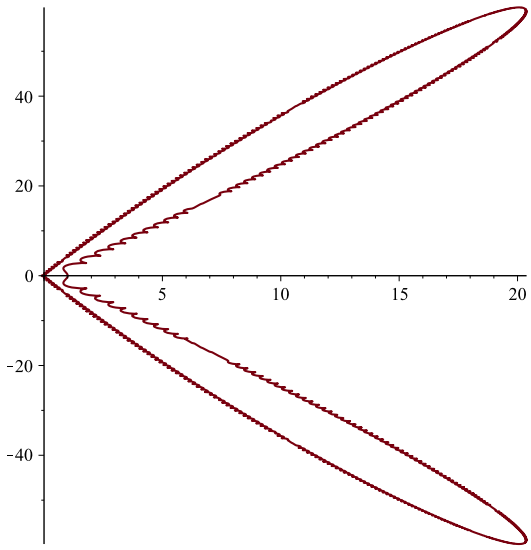

Fig. 38: $(\bar{\mathbb{C}}\backslash F_1(\bar{\mathbb{D}})^*$

13 Generalized Fejér kernels

In analysis there are two types of extremal non-negative polynomials introduced by Fejér. In a closed form they can be written as

$$\Phi_{N-1}^{(1)}(t) = \left(\frac{\cos\frac{N+1}{2}t}{\cos t - \cos\frac{\pi}{N+1}}\right)^2 \quad \text{and} \quad \Phi_{N-1}^{(2)}(t) = \left(\frac{\sin\frac{N}{2}t}{\sin\frac{t}{2}}\right)^2. \tag{19}$$

Graphically these two polynomials look similar; however, there is no explanation of that fact and no relation between these two families polynomials has been established.

Surprisingly, both polynomials turned out to be involved in the problem of optimal stability. It was showed in [16] that the polynomials $\Phi_{N-1}^{(1)}(t)$ play a central role in the problem of 1-cycle (equilibrium) stability, while $\Phi_{N-1}^{(2)}(t)$ are central to the 2-cycle stability.

The family of complex polynomials $q(z, T, 2, 2)$ that we introduced above generates a new family of trigonometric polynomials which contains both Fejér polynomials as particular cases. Denote $q(z, T, 2, 2)$ by $q_N^{(T)}(z)$ in this section, and their coefficients by $a_j^{(T)}$. Let

$$G_{N-1}^{(T)}(t) = \Im\left\{\frac{e^{i\frac{t-\pi}{T}} q_N^{(T)}(e^{it})}{\sin\frac{t-\pi}{T}}\right\},\ 0 < t < \pi.$$

One can check that

$$\frac{1}{G_{N-1}^{(T)}(0+)} \cdot G_{N-1}^{(T)}(t) = \frac{1}{\Phi_{N-1}^{(T)}(0)} \cdot \Phi_{N-1}^{(i)}(t),\ T = 1, 2.$$

Letting $\tau = (t-\pi)/T$ we obtain the normalized version

$$\tilde{G}_{N-1}^{(T)}(\tau) = \frac{1}{\sin\tau}\sum_{j=1}^{N}(-1)^{j-1} a_j^{(T)} \sin(1+(j-1)T)\tau. \tag{20}$$

13.1 Some properties of $\tilde{G}_{N-1}^{(T)}$

Note that

$$a_j^{(T)} = (1+(j-1)T)a_{N-j+1}^{(T)},$$

and that

$$\tau_j = \frac{\pi(N-2j)}{2+(N-1)T}$$

are double roots of $\tilde{G}_{N-1}^{(T)}(\tau)$.

In Fig.39 we display the plots of a few generalized Fejér polynomials (20). T=1 coral, T=2 blue, T=3 green, T=4 red.

The classic Fejér polynomials are plotted for T=1 and T=2, however they are shifted by π and $\pi/2$ correspondently because of the τ substitution. These plots support the following

Conjecture B. *The generalized Fejér polynomials*

$$\sum_{j=1}^{N}(-1)^{j-1} a_j^{(T)} \sin(1+(j-1)T)\tau$$

are non-negative on $[0, \pi]$.

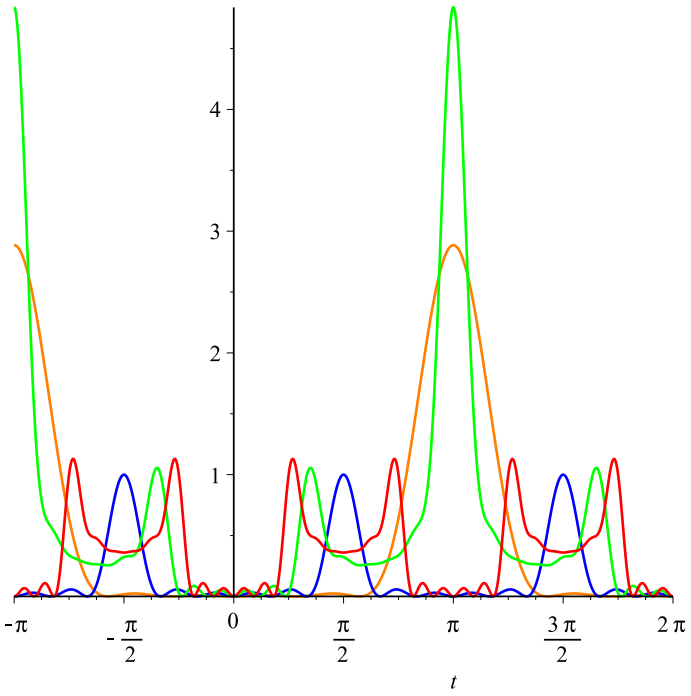

Fig. 39: Graphs of polynomials $\tilde{G}^{(T)}_{N-1}(\tau)$, T=1,2,3,4.

14 Conclusion

We list below what we were able to prove, and what we conjecture to be true.

(i) We were able to find the optimal coefficients for real multipliers in the case of an equilibrium and 2-cycle $T = 1, 2$.

(ii) We were able to find the optimal coefficients for complex multipliers with $\Re(\mu) < 0$ in the case of an equilibrium $T = 1$.

(iii) We have found coefficients for real multipliers in the case of T-cycles, $T \geq 3$, which vastly improve the results obtained by using Alexander polynomials. We conjecture that the discovered coefficients are optimal.

(iv) We have suggested improved coefficients for the complex multipliers with $\Re(\mu) > 0$. We don't know whether they are optimal.

(v) We have found a family of trigonometric polynomials that contains Fejér polynomials as a particular case which we conjecture to be non-negative.

We believe that the developed techniques can also be useful in the attempts to solve the second part of Hilbert's 16th problem, which deals with the number and location of limit cycles of a planar polynomial vector field of degree n. The development of computational sciences made it possible to employ computers in this matter, thus discretizing the problem and reducing it to the problem of detecting of cycles of high periods in discrete settings, which is the topic of this article.

References

1. J. W. Alexander, Functions which map the interior of the unit disc upon simple regions, Ann. of Math. 17 (1915-16), 12–22.
2. S. Bielawski, D. Derozier and , P. Glorieux, Controlling unstable periodic orbits by a delayed continuous feedback, Phys. Rev. E 49, R971 (1994)
3. M. E. Bleich and J. E. S. Socolar, Stability of periodic orbits controlled by time-delay feedback, Phys. Lett. A 210, 87 (1996).
4. S.Boccaletti, C. Grebogi, Y.-C. Lai, H. Mancini, D. Maza, The control of chaos: Theory and applications, Physics Reports, 329 (2000), 103-197
5. T. Dahms, P. Hovel, and E. Scholl, Control of unstable steady states by extended time-delayed feedback, Phys. Rev. E 76, 056201 (2007).
6. B. Fiedler, V. Flunkert, M. Georgi, P. Hövel, and E. Schöll: Refuting the odd number limitation of time-delayed feedback control , Phys. Rev. Lett. 98, 114, 101 (2007).
7. D. J. Gauthier: Resource letter: Controlling chaos, Am. J. Phys. 71, 750 (2003).
8. J. Hizanidis, R. Aust, and E. Scholl: Delay-induced multistability near a globalbifurcation, Int. J. Bifur. Chaos 18, 1759 (2008).
9. P. Hovel and J. E. S. Socolar: Stability domains for time-delay feedback control with latency, Phys. Rev. E 68, 036–206 (2003).
10. P. Hovel and E. Scholl: Control of unstable steady states by time-delayed feedback methods, Phys. Rev. E 72, 046–203 (2005).
11. W. Just, H. Benner, and E. Scholl: Control of chaos by time–delayed feedback: a survey of theoretical and experimental aspects, in Advances in Solid State Phyics, edited by B. Kramer (Springer, Berlin, 2003), vol. 43, pp. 589–603.
12. W. Just, T. Bernard, M. Ostheimer, E. Reibold, and H. Benner: Mechanism of time-delayed feedback control, Phys. Rev. Lett. 78, 203 (1997). Time-Delayed Feedback Control 63.
13. W. Just, B. Fiedler, V. Flunkert, M. Georgi, P. Hovel, and E. Scholl: Beyond odd number limitation: a bifurcation analysis of time-delayed feedback control, Phys. Rev. E 76, 026–210 (2007).
14. D. Dmitrishin, P. Hagelstein, A. Khamitova, A. Stokolos, On the stability of cycles by delayed feedback control, (2014) arXiv:1501.04573. Published online in Linear and Multilinear Algebra, DOI:10.1080/03081087.2015.1102833
15. D. Dmitrishin and A. Khamitova, Methods of harmonic analysis in nonlinear dynamics, Comptes Rendus Mathematique, Volume 351, Issues 9-10, May 2013, 367-370.
16. D. Dmitrishin, A.Khamitova and A.Stokolos, Fejér polynomials and Chaos, Springer Proceedings in Mathematics and Statistics, 108 (2014), pp 49-75.
17. D.Dmitrishin, A.Khamitova, A.Korenovskyi, A.Stokolos, Optimal stabilization of a cycle in nonlinear discrete systems, arXiv:1307.7369 [math.DS]

18. D.Dmitrishin, A.Khamitova and A.Stokolos, On the generalized linear and non-linear DFC in non-linear dynamics, arXiv:1407.6488 [math.DS]
19. D.Dmitrishin, A.Khamitova, A.Stokolos and M. Tohaneanu, Complex polynomials and cycles in nonlinear autonomous discrete dynamical systems, in preparation.
20. R.A.Horn and C. Johnson, Matrix Analysis, Cambridge University Press, 1985, p.561.
21. Ö. Morgül, Further stability results for a generalization of delayed feedback control, Nonlinear Dynamics, 1 August 2012, pp. 1-8.
22. I.D. Murray. Mathematical biology. An introduction. N-Y.: Springer, 3rd., 2002. - 551p.
23. E. Ott, C. Grebogi, J. A. Yorke: Controlling chaos. Phys. Rev. Lett.. 64(11):1196-1199(1990)
24. E. Scholl, P. Hovel, V. Flunkert, M. A. Dahlem, H. Nakajima: On analytical properties of delayed feedback control of chaos, Phys. Lett. A 232, 207 (1997).
25. E. Scholl and H. G. Schuster (Editors): Handbook of Chaos Control (Wiley- VCH, Weinheim, 2008), second completely revised and enlarged edition.
26. A. M. Sharkovsky, Co-Existence of Cycles of a Continuous Mapping of a Line onto itself. Ukrainian Math. Z. 16, 61-71, 1964.
27. J. E. S. Socolar, D. W. Sukow, and D. J. Gauthier: Stabilizing unstable periodic orbits in fast dynamical systems, Phys. Rev. E 50, 32–45 (1994).
28. J. E. S. Socolar and D. J. Gauthier: Analysis and comparison of multiple-delay schemes for controlling unstable fixed points of discrete maps, Phys. Rev. E 57, 65–89 (1998).
29. A. Solyanik, Personal communication.
30. Tian Y.-P., Jiandong Z. Full characterization on limitation of generalized delayed feedback control for discrete-time systems, Phisica D 198, 248-257 (2004)
31. T. Ushio and S. Yamamoto, Prediction-based control of chaos, Phys. Letters A 264 (1999), 30-35.
32. d.S.M. Vieira, A.J. Lichtenberg: Controlling chaos using nonlinear feedback with delay. Phys. Rev. E 54, 1200-1207 (1996)
33. S. Yamamoto, T. Hino and T. Ushio, "Dynamic Delayed Feedback Controllers for Chaotic Discrete-Time Systems," IEEE Transactions on Circuits and Systems I, vol. 48, no. 6, pp. 785-789, 2001.
34. S. Yanchuk, M. Wolfrum, P. Hovel, and E. Scholl: Control of unstable steady states by long delay feedback, Phys. Rev. E 74, 026201 (2006).
35. J.Zhu and Y-P. Tian, Necessare and sufficient condition for stabiilizability of disxrete-time systems via delayed feedback control, Phys. Letters A 343 (2005), 95-107.
36. Tian Y.-P., Jiandong Z. Full characterization on limitation of generalized delayed feedback control for discrete-time systems, Phisica D 198, 248-257 (2004)